Available online at www.sciencedirect.com
ScienceDirect
Polymer 48 (2007) 3162–3169
polymer
www.elsevier.com/locate/polymer

Characterization, magnetic and transport properties of polyaniline synthesized through interfacial polymerization

Panagiotis Dallas, Dimosthenis Stamopoulos, Nicholaos Boukos, Vasilios Tzitzios, Dimitrios Niarchos, Dimitrios Petridis*

NCSR Demokritos, Institute of Materials Science, Patriarhou Grigoriou & Neapoleos, Athens 15310, Greece

Received 8 September 2006; received in revised form 14 February 2007; accepted 23 March 2007
Available online 30 March 2007

Abstract

The present work describes the interfacial polymerization of aniline in the absence or presence of surfactants. Polyaniline was readily obtained in the semi-oxidized doped state and was cast from the aqueous phase. The structural and morphological characteristics of the polyanilines were deduced from X-ray Diffractometry and Scanning Electron Microscopy. Various morphologies were obtained depending on the surfactant addition. Conductivity measurements recorded for HCl doped polyaniline nanoneedles from 5 to 330 K showed a T_c value at 230 K, where their transport behaviour changes from metallic-like above T_c to semiconductive below T_c. Furthermore, extensive magnetic measurements have been performed as a function of applied field and temperature.

Keywords: Interface polymerization; Metallic transport in polymers; Magnetic properties of polymers

1. Introduction

Polyaniline is an important member in the class of electrically conducting polymers due to the easy doping–dedoping process and its thermal and environmental stabilities. The conjugation mechanism of polyaniline is unique among other conducting polymers, owing to a combination of benzenoid and quinoid rings leading to three different oxidation states [1].

Recent advances in the field of polymer science have brought an increasing research interest in nano- or submicron structured conjugated polymers [2]. A current challenge in this field of nanotechnology is to synthesize small enough polymeric nanostructures with almost monodispersed size distribution. Conductive polymeric nanofibers synthesized via an interfacial procedure have been previously reported for polyaniline [3,4]. This method has been also applied for the synthesis of polypyrrole and PPy/Ag nanocomposites [5]. Other synthetic approaches have been also followed for the formation of nanostructural polyaniline [6–9]. The ability of these polymers to detect upon a redox reaction of various molecules, such as glycine [10] or hydrazine [11], gives rise to one of their fundamental applications, i.e. their use as biosensors. Since the conductivity values of polyaniline change by many orders of magnitude upon doping–dedoping, micro- or nanoelectronic sensor devices can be fabricated. However, the design of nanostructured conjugated polymers involves the combination of numerous factors, while slight structural changes induce significant changes in their properties, such as conductivity values. Besides, the transport properties of conjugated polymers are currently a research field of increasing interest [12], and numerous reports examine their electrical and magnetic properties [13]. Moreover, polyaniline exhibits a large spin density so interesting electrical and magnetic properties arise that are highly dependent on the doping level and the structure of the polymer [14]. Specifically, the intrinsic metallic nature of polyaniline has been indicated by the negative dielectric constant values that have been previously reported [15] and furthermore from the metallic behaviour of

* Corresponding author. Tel.: +30 2106503343; fax: +30 2106519430.
E-mail address: dpetrid@ims.demokritos.gr (D. Petridis).

0032-3861/$ - see front matter © 2007 Elsevier Ltd. All rights reserved.
doi:10.1016/j.polymer.2007.03.055

temperature dependent resistivity data [16]. Additionally, ferromagnetic interactions of the spins were revealed by EPR measurements [17]. These spins are mainly localized on nitrogen atoms but to some extend are also delocalized on phenyl rings giving rise to a significant Pauli susceptibility [18]. Concerning the electrical properties of conductive polymers, recently, in highly conductive polyaniline the resistivity was observed to decrease monotonically as the temperature was lowered down to 5 K, while the infrared spectra were characteristic of the conventional Drude model even at the lowest frequencies measured [19].

In this article we present our results concerning an interfacial polymerization leading to the formation of polyaniline nanostructures. The main advantages of the interfacial polymerization compared to the conventional polymerization in aqueous solution are the slow reaction rate resulting in nanostructures with a narrow size distribution and the ability to add various surfactants either organophilic or hydrophilic in the aqueous or in the organic solvent. A metallic behaviour from 330 to 230 K was revealed by the temperature variation of resistance, while the magnetic response of the HCl doped polyaniline showed a gradual transition from diamagnetism to paramagnetism as the temperature was lowered from 330 to 10 K.

2. Experimental part

2.1. Reagents

Aniline monomer and ammonium peroxydisulfate were purchased from Riedel De Haan, while hydrochloric acid from Merck. H_2O_2 was a product of Riedel De Haan. The surfactant molecules, sodium dodecylsulfate and dodecyltrimethylammonium bromide, were products of Aldrich and Merck, respectively.

2.2. Synthesis of polyaniline without surfactants

The polymerization of aniline was conducted in the interface of two immiscible solvents (water/chloroform). The byproducts of the reaction are easily separated due to their solubility in the aqueous or the organic solvents. The polymerization was conducted without stirring and the temperature was 25 °C. To a solution of 0.5 ml aniline monomer (5.2 mmol) in chloroform (total volume 15 ml) were slowly added an acidic aqueous solution made up of 13 ml H_2O, 2 ml HCl, 1.2 g ammonium peroxydisulfate (5.2 mmol) as an oxidizing agent and 3 drops of H_2O_2 (30%). The protonated green colored emeraldine salt of polyaniline was obtained after 8 h of polymerization. It was isolated by centrifugation, washed several times with water and dried.

2.3. Synthesis of polyaniline in the presence of surfactants

The same procedure was followed but the interfacial polymerization was conducted in the presence either of cationic surfactant, 89 mg of dodecyltrimethylammonium bromide (0.7 mmol), or of an anionic surfactant, 80 mg of sodium dodecylsulfate (0.7 mmol). The surfactants were added to the organic phase and the polyanilines obtained are denoted as pani/DTAB and pani/SDS, respectively. In both cases the reaction temperature, the reagents and their concentration were the same as above.

3. Characterization of the samples

All samples were dried at 60 °C for 24 h prior to measurements in order to evaporate any remained solvent. X-ray diffraction (XRD) patterns were recorded for the structural characterization of the polyanilines on powder samples by a Siemens 500 Diffractometer with a scan rate 0.03° per second. Infrared (FT-IR) spectra (Aldrich, 99%, FT-IR grade) were obtained from a Bruker Equinox 55/S model spectrometer (KBr pellets). UV–visible spectra were measured from aqueous or organic solutions on a Shimadzu 2100 spectrometer. SEM images were recorded on a FEI Inspect apparatus. Resistivity and magnetization measurements were performed by means of a Superconductive Quantum Interference Device (SQUID) system. The polymer was pressed into pellets under pressure (3 MPa) and the measurements were performed in the standard four points configuration with silver paste contacts. ζ-Potential measurements were carried out in a Malvern-Zetasizer instrument in aqueous solutions. Thermogravimetric (TGA) measurements were performed on a Perkin–Elmer Pyris TGA under air flow with a scan rate 10 °C/min. The weight loss due to remained solvent was calculated to be about 2% at 110 °C for the pani/HCl sample.

4. Results and discussion

4.1. Spectroscopic characterization

Interfacial polymerization was conducted in a water/chloroform biphase system, with HCl, ammonium peroxydisulfate and H_2O_2 in the aqueous phase. Following addition of the reactants the interfacial reaction was soon initiated and in a few hours the polyaniline that was formed at the interface rapidly migrated to the aqueous phase. Even though polyaniline is not highly soluble in either polar or organic solvents, in water it forms a stable over a few days dispersion and can be completely solubilized in larger quantities of water. In general conjugated polymers suffer from low solubility in organic or polar solvents [20]. It is known that stable colloidal dispersion formed if the ζ-potential value of the particles is higher than 20 mV. The low ζ-potential values observed for the samples (pani/HCl = +7.4 mV, pani/SDS = −10.1 mV, pani/DTAB = +6.5 mV) justify the low solubility of the polymeric samples (the ζ-potential diagrams are given in Supplementary data).

The UV–visible spectra of the three green polyaniline salts (pani/HCl, pani/DTAB, pani/SDS) measured from water solution are shown in Fig. 1. The spectra show three absorption bands at 360–370 nm (π–π* transitions), 410–440 nm

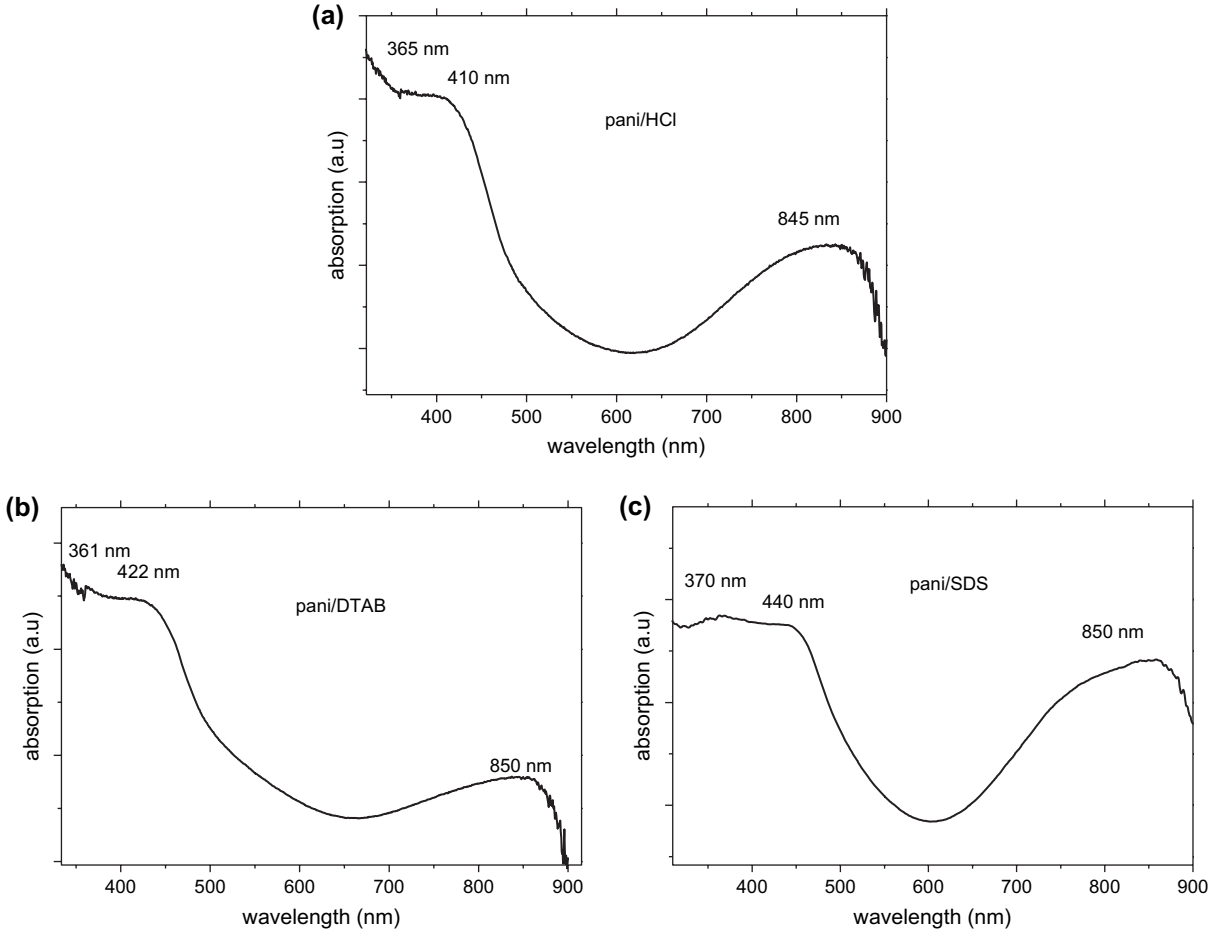

Fig. 1. UV–visible spectra recorded from aqueous solutions of (a) pani/HCl; (b) pani/DTAB; (c) pani/SDS.

(low wavelength polaron band) and 840–850 nm (high wavelength polaron band) [21,22]. The UV results combined with the FT-IR spectra to be later discussed drive to the conclusion that the polymer is in the conductive state. No significant differences were observed in the three spectra, indicating that, irrespective of the presence or not of surfactants, the oxidation states of the polymers are similar.

We must also note that during the interfacial polymerization a small amount of non-doped polyaniline is transferred to the organic phase giving a purple-blue color. The presence of a polyaniline fraction in the organic phase can be detected by the UV–visible spectrum (Fig. 2). The spectrum shows the characteristic absorption of the non-doped oxidized emeraldine base, meaning that a non-protonated fraction of polyaniline migrated to chloroform [23,24].

The IR spectra of the polyanilines shown in Fig. 3 indicate that the polymers exist in the doped semi-oxidized state [25]. The absorptions at 1575 and 1495 cm^{-1} correspond to the stretching vibration of the quinoid and benzenoid rings and these at 1319 and 1211 cm^{-1} to the C–N and C=N stretching modes and appear at exactly the same wavenumbers for the three samples. The previously mentioned peaks indicate that the polymers are in the doped form. The vibrations from the aliphatic chains of the surfactants are observed at 2921 and 2850 cm^{-1} for the pani/SDS sample while the C–H of the aromatic ring is clearly seen at 3030 cm^{-1}. Finally, the –N–H vibrational modes are located in the 3200–3300 cm^{-1} region.

In Fig. 3b the thermogravimetric analysis diagrams are presented. As it has been previously reported the HCl doped

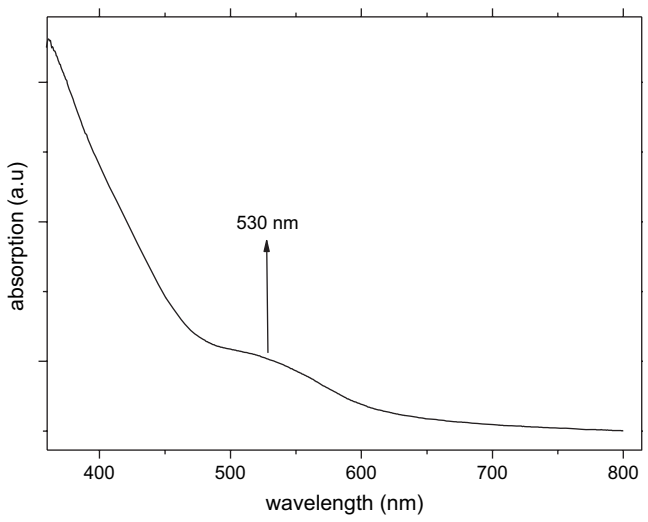

Fig. 2. UV–visible spectrum of the chloroform phase indicating the presence of non-doped emeraldine base form. Sample: pani/HCl.

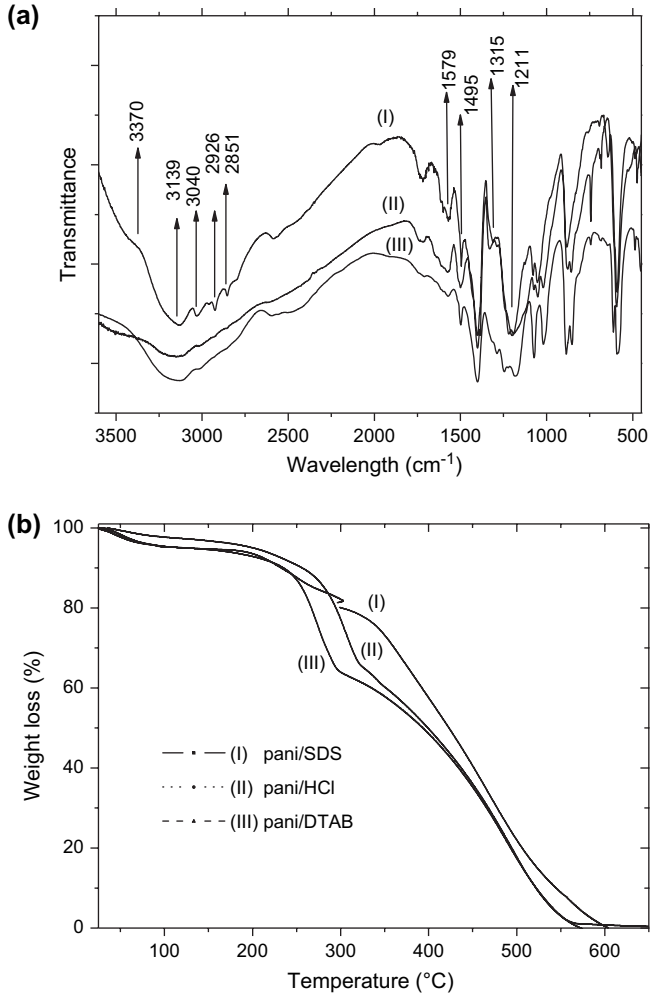

Fig. 3. (a) FT-IR spectra of the polyaniline samples (I) pani/SDS, (II) pani/DTAB, (III) pani/HCl; (b) TGA diagrams.

polyaniline is exhibiting poor thermal stability at higher than 250 °C temperatures. This is what we observe for the pani/HCl and pani/DTAB samples. In contrast, the pani/SDS sample, where the DS^- acting as counterions exhibits the lower weight loss above 250 °C. The thermal stability of doped pani is known to improve after using organic acids as dopants [26].

4.2. Morphology and crystal structure

Concerning the crystal structure of the polyaniline samples, the XRD patterns reveal that pani/SDS and pani/DTAB are amorphous polymers, with the central broad band centered at $2\theta = 24°$ to be characteristic of a disordered structure (Fig. 4). In this instance the large surfactant molecules do not favor an ordered structure for polyaniline. This broad amorphous background is also observed in pani/HCl sample which, however, exhibits a partial crystallinity as it is indicated by the diffraction peaks at $2\theta = 19°$ and $2\theta = 25.5°$. The latter diffraction peak (d-spacing = 3.5 Å) implies that the phenyl rings are densely packed [27] giving rise to a planar conformation and thus to an extensive interchain $\pi-\pi^*$ orbitals overlap.

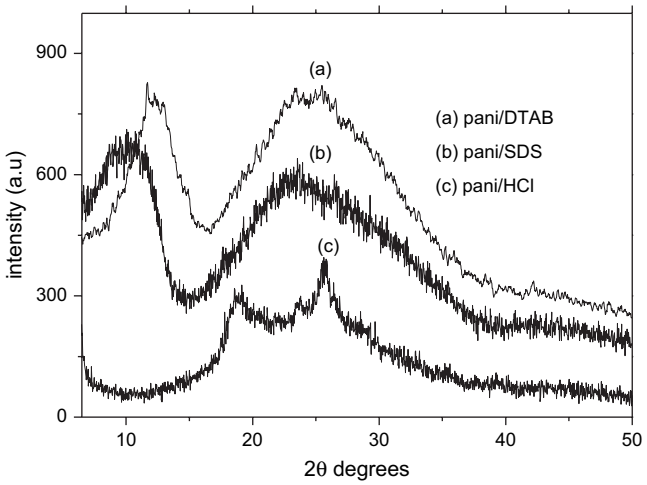

Fig. 4. X-ray diffraction patterns for the polyaniline samples (a) pani/DTAB; (b) pani/SDS; (c) pani/HCl.

Furthermore, the increased crystallinity indicates a high doping level [27c].

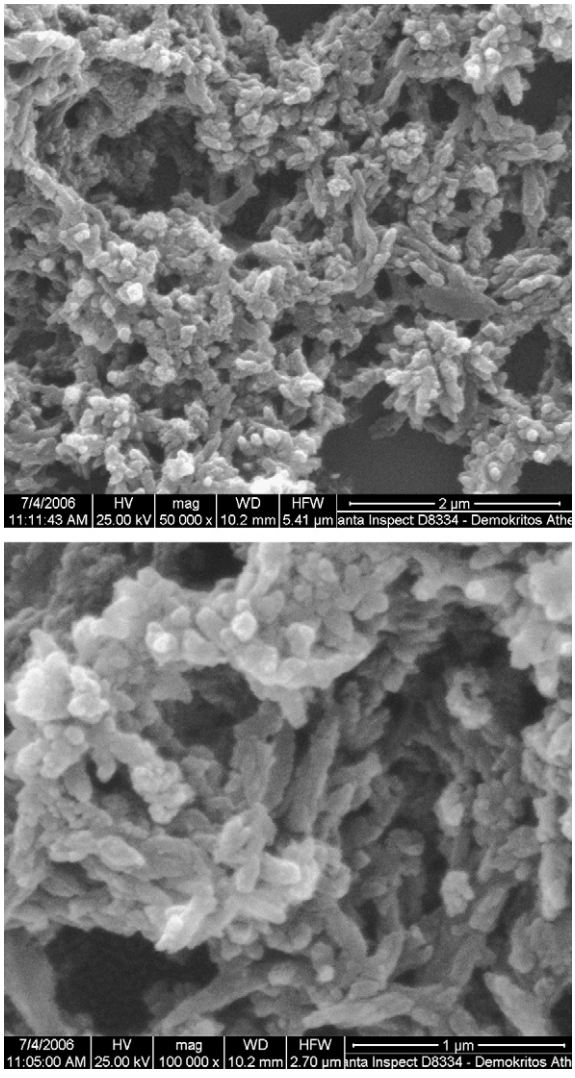

Fig. 5. SEM images of pani/DTAB.

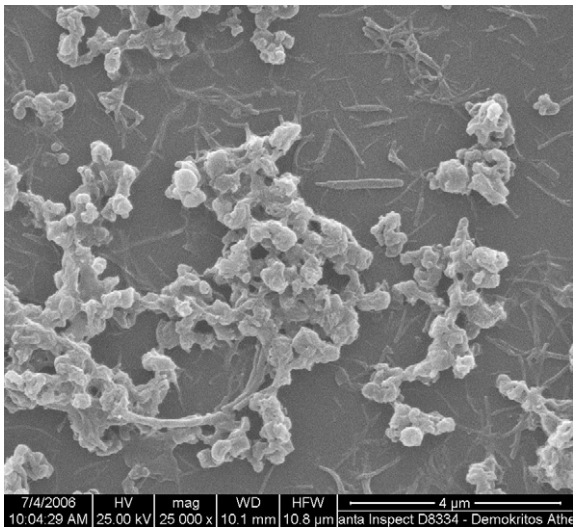

Fig. 6. SEM images of pani/SDS.

The morphological characteristics of the polymers were examined by Scanning Electron Microscopy. SEM images of the pani/DTAB (Fig. 5) show that the polymer forms slightly elongated structures, very close to spheres, with a mean diameter 100–150 nm. A rather uniform size distribution is observed which is attributed to the formation of isolated and of uniform size surfactant islands. These islands arise from the orientation of surfactant molecules at the interface, with the polar group headed to the aqueous phase and the organophilic aliphatic chain to the organic phase. Polymerization in the constrained space of these templates resulted in nearly spherical polyaniline particles with a low mean diameter and narrow size distribution.

Pani/SDS is growing mostly in a similar with pani/DTAB spherical shape, but also a low percentage of nanofibers is observed (Fig. 6). The presence of the two different structures may be also due to the binary role of the anionic surfactant that acts either as a template or as a counterion. The fraction of DS^- that forms templates probably leads to spherical shaped particles in the same manner as DTAB, while DS^- acts as a balancing anion it is incorporated in the polymer chains [28] and favors the fibrillar morphologies.

Pani/HCl forms exclusively nanoneedles and nanofibers with a mean diameter of about 80 nm. Their length varied from 400 nm to 2 µm (Fig. 7). The linear, fibrillar morphology is highly favored and no other morphologies are observed in contrast with the polyanilines synthesized through a surfactant mediated polymerization. In all cases, the uniform size distribution of the resulting nanostructures and the very narrow mean diameter demonstrate the importance of the slow and

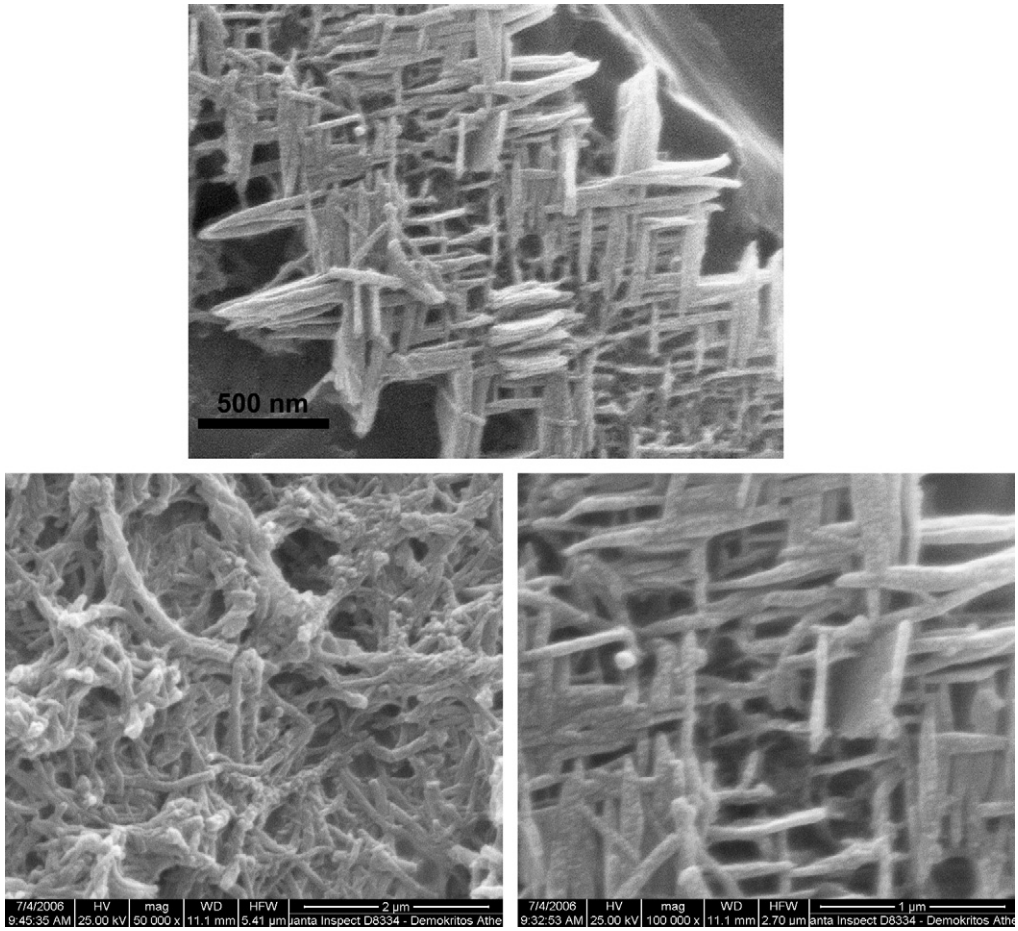

Fig. 7. SEM images of pani/HCl.

controllable interfacial polymerization in the restricted two-dimensional space of the water–chloroform interface.

4.3. Transport and magnetic properties of sample pani/HCl

We have studied the dc conductivity and the magnetic properties of the pani/HCl sample which has been synthesized in the absence of insulating components like surfactants and exhibits a partial crystallinity in the temperature range from 5 to 330 K. The applied current is 10 nA in zero field. In Fig. 8 are presented the respective data in the form of conductivity. From 330 to 230 K a typical metallic-like behaviour is indicated by the increase in the conductivity upon decreasing the temperature. The XRD pattern of the sample indicated the formation of a mostly amorphous polymer, however, a π orbitals' overlap is indicated by the diffraction peak at $d = 3.5$ Å. This overlap is reported to facilitate the charge transfer and thus in our case the response appears metallic down to $T = 230$ K and becomes semiconducting at lower temperatures [19]. This implies that below this temperature the electrons are localized and the charge transport follows the variable range hopping mechanism as it has been proposed by Mott and David [29]. The observed metal-semiconducting transition is expected due to Peierls instability which demonstrates that 1-D conductors are intrinsically unstable [30]. The metallic transport behaviour is proposed to arise from a spin delocalization which is later identified by the magnetic measurements, while the T_c value of 230 K is in good agreement with previous works [31]. A significant decrease in conductivity is observed below 50 K with values higher than the measuring range of the voltameter apparatus. The absolute value of conductivity at room temperature is near 10^{-1} S/cm.

In order to study in more detail the electrical behaviour of the sample we plotted the resistance values in the semiconducting region following the Mott relation: $\ln(R_T/R_{330})$ vs $1/T^{1/2}$, Fig. 8b. The polymer is considered as 1-D conductor ($x = 1/2$). The fitting of the resistance data with this relation yields a linear plot. The Mott temperature, reflecting the energy required for charge hopping, is derived from the slope and it is calculated to be 1.5×10^4 K [32].

The magnetization vs applied magnetic field of the pani/HCl sample was recorded in various temperatures from 330 to 10 K. Detailed curves are presented in Fig. 9. A paramagnetic behaviour with a constant increase in the magnetization

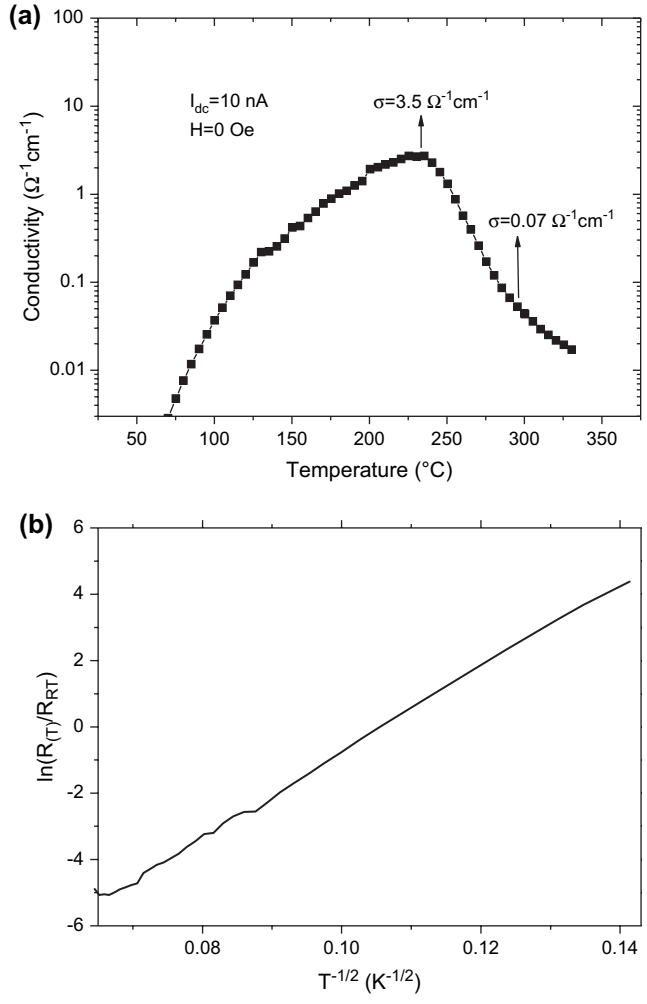

Fig. 8. (a) Representative conductivity measurement from 50 to 330 K for pani/HCl; (b) The resistivity data from 50 to 230 K are plotted according to Mott relation setting $x = 1/2$ (1-D semiconductor), leading to a linear fit.

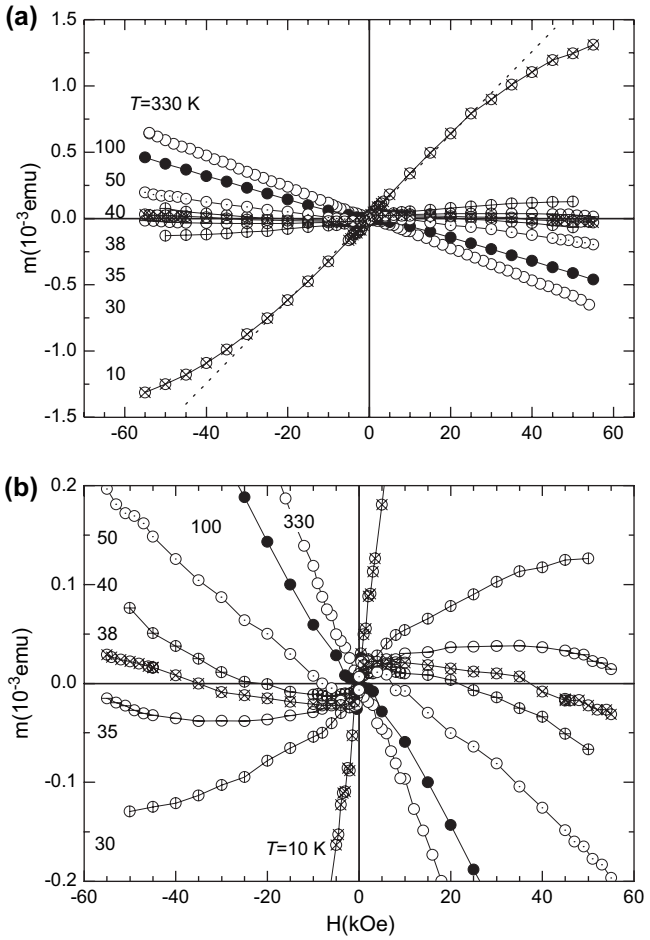

Fig. 9. Magnetization data for pani/HCl recorded at various temperatures from $T = 10$ to $T = 330$ K.

was observed in 10 K, which gradually changes to diamagnetic as the temperature increases. We consider this transition to arise from electron localization in low temperatures. The diamagnetic behaviour is associated with the metallic response meaning that a spin delocalization occurs and a typical metallic diamagnetism is observed. In lower temperatures the spins are freezing, the system suffers from the Peierls instability, and thus the electrons are localized giving rise to a metal-semiconducting transition and an associated paramagnetism. At all temperatures the *m*(H) curves exhibit a clear curvature that starts to form in the high field region, indicative of a tendency of the sample to become diamagnetic at very high magnetic fields. Finally, no remnant magnetization is observed at any temperatures. These results are in good agreement with a model that considers the spins as located mainly at the nitrogen atoms and in some degree delocalized on phenyl rings as it has been previously proposed from EPR and magnetic susceptibility measurements [17,18]. A similar connection of electron delocalization with high temperature diamagnetism and a disordered phase with low temperature paramagnetism has been recently observed in graphite filaments [33]. The high diamagnetic susceptibility of carbon nanostructures is linked to an increased ordering and consequently to an electron delocalization, while it is well known that aromatic molecules exhibit a weak diamagnetism [33b].

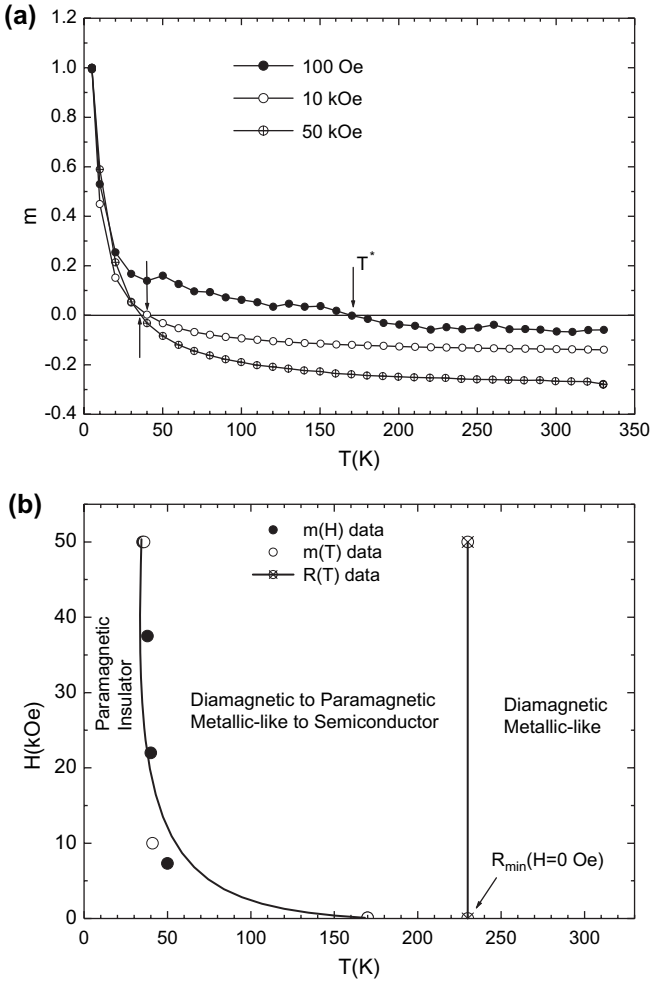

Fig. 10. (a) *m* vs *T* curves under different applied magnetic fields (100 Oe/10 kOe/50 kOe); (b) The diagram summarizes the magnetic and electrical data from 5 to 330 K.

Furthermore, the temperature dependence of magnetization is following a Curie-type curve and indicates the transition from diamagnetism to paramagnetism (Fig. 10). The increase of magnetization in low temperatures is in accordance with a typical Curie-type temperature dependence of susceptibility [34]. The temperature where the transition to diamagnetism occurs is depending on the applied magnetic field and is shifted to lower temperatures as the intensity of the magnetic field increases. Specifically, under 100 Oe applied field the transition temperature is 170 K and in 10 and 50 kOe is 40 and 39 K, respectively. The field dependent transition is assigned to inhibited electron localization due to the very high external magnetic field which facilitates the electron delocalization.

5. Conclusions

This paper described the interfacial polymerization of aniline, its assembly to various nanostructures and its electrical and magnetic properties. The SEM images reveal the growth of polyaniline fibrillar nanostructures in the absence of surfactants, while nearly spherical shaped nanoparticles are obtained when a surfactant was added. A metallic behaviour is observed at temperatures above 230 K for pani/HCl sample with a gradual transition from a diamagnetic to a paramagnetic behaviour as the temperature was lowered. We assign these transitions to spin localization while the temperature is decreased. Below 230 K the current transport follows a typical variable range hopping mechanism.

Appendix. Supplementary data

ζ-Potential measurements for all samples are presented in Supplementary data. Supplementary data associated with this article can be found in the online version, at doi:10.1016/j.polymer.2007.03.055.

References

[1] Huang WS, Humphrey BD, MacDiarmid AG. J Chem Soc Faraday Trans 1986;82:2385.
[2] Huang J, Virji S, Weiller B, Kaner R. J Am Chem Soc 2003;125:314.
[3] Huang J, Kaner RB. J Am Chem Soc 2004;126:851.
[4] Li W, Wang HS. J Am Chem Soc 2004;126:2278.
[5] Dallas P, Niarchos D, Vrbanic D, Boukos N, Pejovnik S, Trapalis C, et al. Polymer 2007;48(7):2007–13.
[6] Wu CG, Bein T. Science 1994;264:1757.
[7] (a) Martin CR. Chem Mater 1996;8:1739;
(b) Wang CW, Wang Z, Li MK, Li HL. Chem Phys Lett 2001;341:431.
[8] (a) Qiu HJ, Wan MX. J Polym Sci Part A Polym Chem 2001;39:3485;
(b) Yang YS, Wan MX. J Mater Chem 2002;12:897.
[9] Huang LM, Wang ZB, Wang HT, Cheng XL, Mitra A, Yan YX. J Mater Chem 2002;12:388.
[10] Sukeerthi S, Contractor AQ. Anal Chem 1999;71:2231.
[11] Virji S, Huang J, Kaner RB, Weller BH. Nano Lett 2004;4:491.
[12] Aleshin AN. Adv Mater 2006;18:17.

[13] Santos MC, Bredas JL. In: Merhing M, Roth S, editors. Electronic properties of conjugated polymers. Berlin: Springer Verlag; 1989.
[14] Mizobushi H, Kawai T, Yoshino K. Solid State Commun 1995;96:925.
[15] (a) Joo J, Wang YZ, Kaneko H, Ishiguro T, Tsukamoto J. Synth Met 1995;69:69;
(b) Soares BG, Leyva ME, Barra GM, Khastgir D. Eur Polym J 2005; 42:676.
[16] Joo J, Oblakowski Z, Du G, Pouget JP, Oh EJ, Wiesinger JM, et al. Phys Rev B 1994;49:2977.
[17] Yoshizawa K, Tanaka K, Yamabe T. J Chem Phys 1992;96:5516.
[18] Jozefowicz ME, Laversanne R, Javadi HHS, Epstein AJ, Pouget JP, Tang X, et al. Phys Rev B 1989;39:12958.
[19] Lee K, Cho Sh, Park SH, Heeger AJ, Lee ChW, Lee SH. Nature 2006;41:65.
[20] Bae WJ, Kim KH, Jo WH. Macromolecules 2005;38:1044.
[21] Xia Y, Wiesinger JM, MacDiarmid AG. Chem Mater 1995;7:443.
[22] Davey JM, Too CO, Ralph StF, Maguire LK, Wallace GC. Macromolecules 2000;33:7044.
[23] (a) Hatchett DW, Josowicz M, Janata J. J Phys Chem B 1999;103: 10992;
(b) MacDiarmid AG, Epstein A. Synth Met 1995;69:85.
[24] Chan HSO, Ho PKH, Ng SC, Tan BTG, Tan K. J Am Chem Soc 1995;117:8517.
[25] Albuquerque JE, Mattoso LHC, Balogh DT, Faria RM, Masters JG, MacDiarmid AG. Synth Met 2000;113:19.
[26] Konyushenko EN, Stejskal J, Trchova M, Hradil J, Kovarova J, Prokes J, et al. Polymer 2006;47:5715.
[27] (a) Luzny W, Sniechowski M, Laska J. Synth Met 2002;126:27;
(b) Stejskal J, Riede A, Hlavata D, Prokes J, Helmstedt M, Holler P. Synth Met 1998;96:55;
(c) Pouget JP, Josefowicz ME, Epstein AJ, Tang X, MacDiarmid AG. Macromolecules 1991;24:779;
(d) Mazerolles L, Folch S, Colomban Ph. Macromolecules 1999;32:8504.
[28] Omastova M, Trchova M, Kovarova J, Stejskal J. Synth Met 2003; 138:447.
[29] Mott NF, David EA. Electronic processes in non-crystalline materials. Oxford: Oxford University Press; 1979.
[30] Ku CC, Liepins R. Electrical properties of polymers. Hanser Publishers; 1987.
[31] Zhang Zh, Wei Zh, Wan M. Macromolecules 2002;35:5937.
[32] (a) Reghu M, Cao Y, Moses D, Heeger AJ. Phys Rev B 1993;47:1758;
(b) Wang YZ, Joo J, Hsu CH, Epstein AJ. Synth Met 1995;69:267;
(c) Wang YZ, Joo J, Hsu CH, Epstein AJ. Synth Met 1995;68:207.
[33] (a) Calderon-Moreno JC, Labarta A, Batlle X, Crespo D, Pol VG, Pol SV, et al. Carbon 2006;44:2849;
(b) Shibayama Y, Sato H, Enoki T. Phys Rev Lett 2000;84(8):1744;
(c) Wabayashi K, Fujita M, Ajiki H, Sigrist M. Phys Rev B 1999;59(12): 8271.
[34] Chaudhuri D, Kumar A, Sarma DD, Garcia Hernadez M, Joshi JP, Bhat SV. Appl Phys Lett 2003;82:1733.